Enhancement of unidirectional transmission through the coupling of nonlinear photonic crystal defects

Xu-Sheng Lin, Wei-Qing Wu, Hui Zhou, and Kai-Feng Zhou

Department of Physics, Shantou University, Shantou 515063, China
xslin@stu.edu.cn

Sheng Lan

Laboratory of Photonic Information Technology, School for Information and Optoelectronic Science and Engineering, South China Normal University, Guangzhou 510631, China

Abstract: We investigate the unidirectional transmission behavior of coupled photonic crystal defects with nonlinearity by using the coupled mode theory, focusing on how to enhance the transmission contrast. Although the unidirectional transmission originates from the asymmetric configuration and nonlinear property of the structure, it is revealed that the maximum transmission contrast depends mainly on two linear factors. For two coupled defects, they are the highest order of the frequency detuning appearing in the transmission formula and the frequency splitting due to the coupling. Our analyses are supported by the numerical simulations based on the finite-difference time-domain technique. An enhancement of the maximum transmission contrast by an order of magnitude is achieved in the structure consisting of two coupled defects.

OCIS codes: (230.4320) Nonlinear devices; (230.1150) All-optical devices

References and links

1. E. Centeno and D. Felbacq, "Optical bistability in finite-size nonlinear bidimensional photonic crystals doped by a microcavity," Phys. Rev. B **62,** R7683-R7686 (2000).
2. M. Soljacic, M. Ibanescu, S. G. Johnson, Y. Fink, and J. D. Joannopoulos, "Optimal bistable switching in nonlinear photonic crystals," Phys. Rev. E **66,** 055601 (2002).
3. S. Mingaleev and Y. Kivshar, "Nonlinear transmission and light localization in photonic crystal waveguides," J. Opt. Soc. Am. B **19,** 2241-2249 (2002).
4. M. Soljacic, C. Luo, and J. D. Joannopoulos, "Nonlinear photonic crystal microdevices for optical integration," Opt. Lett. **28,** 637-639 (2003).
5. M. F. Yanik, S. Fan, and M. Soljacic, "High-contrast all-optical bistable switching in photonic crystal microcavities," Appl. Phys. Lett. **83,** 2739-2741 (2003).
6. M. F. Yanik, H. Altug, J. Vuckovic, and S. Fan, "Submicrometer all-optical digital memory and integration of nanoscale photonic devices without isolators," J. Lightwave Technol. **22,** 2316-2322 (2004).
7. H. A. Haus, Waves and Fields in Optoelectronics (Prentice-Hall, Englewood Cliffs, NJ, 1984).
8. M. Scalora, J. P. Dowling, C. M. Bowden, and M. J. Bloemer, "The photonic band edge optical diode," J. Appl. Phys.**76,** 2023-2026 (1994).
9. K. Gallo and G. Assanto, "All-optical diode in a periodically poled lithium niobate waveguide," Appl. Phys. Lett. **79,** 314-316 (2001).
10. S. Pereira, P. Chak, J. E. Sipe, L. Tkeshelashvili, and K. Busch, "All-optical diode in an asymmetrically apodized Kerr nonlinear microresonator system," Photonics and Nanostructure-Fundamentals and Applications **2,** 181-190 (2004).
11. M. W. Feise, I. V. Shadrivov, and Y. S. Kivshar, "Bistable diode action in left-handed periodic structures," Phys. Rev. E **71,** 037602 (2005).
12. J. Hwang, M. H. Song, B. Park, S. Nishimura, T. Toyooka, J. W. Wu, Y. Takanishi, K. Ishikawa, and H. Takezoe, "Electro-tunable optical diode based on photonic bandgap liquid-crystal heterojunctions," Nature Materials **4,** 383-387 (2005).

#10367 - $15.00 USD Received 20 January 2006; revised 6 March 2006; accepted 6 March 2006

13. X. S. Lin and S. Lan, "Unidirectional transmission in asymmetrically confined photonic crystal defects with Kerr nonlinearity," Chin. Phys. Lett. **22**, 2847-2850 (2005).
14. S. Lan, X. W. Chen, J. D. Chen, and X. S. Lin, "Physical origin of the ultrafast response of nonlinear photonic crystal atoms to the excitation of ultrashort pulses," Phys. Rev. B **71,** 125122 (2005).
15. S. Fan, P. R. Villeneuve, and J. D. Joannopoulos, M. J. Khan, C. Manolatou, and H. A. Haus, "Theoretical analysis of channel drop tunneling processes," Phys. Rev. B **59,** 15882-15892 (1999).
16. Y. Xu, Y. Li, R. K. Lee, and A. Yariv, "Scattering-theory analysis of waveguide-resonator coupling," Phys. Rev. E **62,** 7389-7404 (2000).
17. Y. Akahane, T. Asano, H. Takano, B.-S. Song, Y. Takana, and S. Noda, "Two-dimensional photonic-crystal-slab channel-drop filter with flat-top response," Opt. Express **13,** 2512-2530 (2005), http://www.opticsexpress.org/abstract.cfm?URI=OPEX-13-7-2512.
18. C. Jin, S. Fan, S. Han, and D. Zhang, "Reflectionless multichannel wavelength demultiplexer in a transmission resonator configuration," IEEE J. Quantum Electron. **39,** 160-165 (2003).
19. B. Maes, P. Bienstman, and R. Baets, "Switching in coupled nonlinear photonic-crystal resonators," J. Opt. Soc. Am. B **22,** 1778-1784 (2005).
20. X. S. Lin, X. W. Chen, and S. Lan, "Investigation and modification of coupling of photonic crystal defects," Chin. Phys. Lett. **22**, 1698-1701 (2005).
21. M. Qiu, "Effective index method for heterostructure-slab-waveguide-based two-dimensional photonic crystals," Appl. Phys. Lett. **81,** 1163-1165 (2002).
22. A. Taflove and S. C. Hagness, Computational Electrodynamics (Artech House, Norwood, MA, 2000). In this paper, a commercial software developed by Rsoft Design Group (http://www.rsoftdesign.com) is used for nonlinear FDTD simulation.

1. Introduction

Over the past few years, the optical bistability in nonlinear photonic crystal (PC) defects has attracted considerable attention because many key components for all-optical signal processing such as switches, transistors, logical gates, and memories can be developed based on it [1-6]. Due to the complexity of the nonlinear processes, simple and efficient analytical tools are highly desirable for understanding the physical mechanisms that govern these nonlinear phenomena. Soljacic et al. firstly described the bistability of a PC defect with Kerr nonlinearity based on the perturbation approximation and the coupled mode theory (CMT) [2,7]. The method they employed makes the bistable phenomenon of nonlinear PC defects easy to understand because only three parameters with clear physical meanings are involved.

It is expected that a PC structure with asymmetric configuration and nonlinearity will act as an optical diode that transmits light of given frequency and power unidirectionally. In the last decade, Scalora et al. suggested the first PC-based optical diode in which the distribution of the linear refractive index is asymmetric. Consequently, the shift of the band edge depends strongly on the incident direction [8]. Several years ago, Gallo et al. demonstrated an all-optical diode in a $LiNiO_3$ grating. There, a phase shift is introduced at an asymmetric position, making the transition between the second harmonic and basic waves waveguiding-direction-dependent [9]. In addition, Mingaleev et al. constructed an optical diode in a line-defect waveguide where four nonlinear PC defects are arranged in an asymmetric fashion [3]. Pereira et al. showed numerically that a structure composed of two channel waveguides side-coupled by a string of circular microresonators can serve as an all-optical diode, if only the coupling between the left-most microresonator and the waveguide is changed a little intentionally [10]. Very recently, Feise et al. investigated the bistable diode action in an asymmetric multi-layer structure where left-handed materials are employed [11]. Meanwhile, an electro-tunable optical diode based on the liquid-crystal heterojunctions was realized in laboratory [12]. These theoretical and experimental investigations provide very important information for the design and improvement of PC-based optical diodes. Unfortunately, the transmission contrast, which is a key index of optical diodes, is not large enough for practical applications in general. Thus, how to enhance the transmission contrast of PC-based optical diodes becomes very urgent.

In our previous study, we have investigated the unidirectional transmission of an asymmetrically confined PC defect and indicated the existence of an upper limit for the transmission contrast of the resulting optical diode based on the CMT and numerical simulations [13]. In this paper, we report on the significant enhancement of the transmission

#10367 - $15.00 USD Received 20 January 2006; revised 6 March 2006; accepted 6 March 2006

contrast of PC-based optical diodes by properly coupling PC defects. The paper is organized as follows. In Section 2, the unidirectional transmission of a nonlinear PC defect that is asymmetrically confined is discussed by using the CMT. Then, we focus on the issue of how to enhance the transmission contrast in Section 3. In Section 4 and 5, we simulate respectively the linear and unidirectional transmission behaviors of the single PC defect and coupled PC defects based on the finite-difference time-domain (FDTD) method and compare the results with the analytical one obtained by the CMT. Finally, a brief summary is given in the conclusion.

2. Description of unidirectional transmission based on the CMT

First of all, we describe the unidirectional transmission of a nonlinear PC defect in the framework of the CMT. A simple example is shown in Fig. 1(a) where a finite PC structure is formed by periodically drilling seven identical air holes in a slab waveguide with Kerr nonlinearity. The PC defect is introduced by increasing the distance between the third and the fourth air holes from a (the lattice constant) to 1.35a. Obviously, the defect is confined asymmetrically. If we denote the decay rates of the mode amplitude into the left and right waveguides as γ_1 and γ_2, and the intrinsic decay rate of the mode amplitude as γ_0, then the total decay rate of the mode amplitude γ is given by ($\gamma_1 + \gamma_2 + \gamma_0$). Based on the CMT, the dynamical equations for the mode amplitude A of the input wave launched from the left side reads

$$\begin{cases} \dfrac{\mathrm{d}A}{\mathrm{d}t} = \left[j\left(\omega_0 - \gamma \dfrac{|s_{\mathrm{out}}|^2}{p_0} \right) - \gamma \right] A + \sqrt{2\gamma_1}\, s_{\mathrm{in}}, \\ s_{\mathrm{out}} = \sqrt{2\gamma_2}\, A \end{cases} \tag{1}$$

where s_{in} and s_{out} are the field amplitudes of the input and output waves, ω_0 is the resonant frequency of the defect mode, and p_0 is the characteristic power that reflects the nonlinear Kerr effect and the spatial confinement of the field in the defect region [2]. Here, the nonlinear shift of the defect mode ($-\gamma|s_{\mathrm{out}}|^2/p_0$) [2] has been taken into account. Based on Eq. (1), the relationship between s_{out} and s_{in} can be derived as

$$\frac{\mathrm{d}s_{\mathrm{out}}}{\mathrm{d}t} = \left[j\left(\omega_0 - \gamma \frac{|s_{\mathrm{out}}|^2}{p_0} \right) - \gamma \right] s_{\mathrm{out}} + \sqrt{4\gamma_1\gamma_2}\, s_{\mathrm{in}}. \tag{2}$$

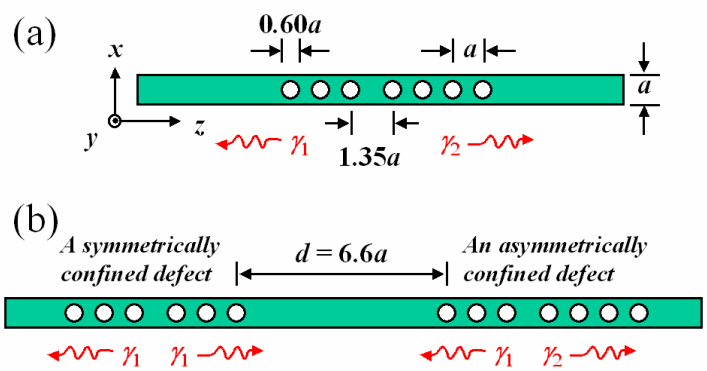

Fig. 1. Schematic structures for the nonlinear PC defects studied in this paper. (a) a single asymmetrically confined PC defect; (b) two coupled PC defects.

By using the steady solution of Eq. (2), the transmission through the PC defect can be derived as

#10367 - $15.00 USD Received 20 January 2006; revised 6 March 2006; accepted 6 March 2006

$$T = \left|\frac{s_{\text{out}}}{s_{\text{in}}}\right|^2 = \frac{p_{\text{out}}}{p_{\text{in}}} = \frac{\eta}{1+\left(p_{\text{out}}/p_0 - \delta\right)^2}, \tag{3}$$

where p_{in} and p_{out} are the input and output powers, $\eta = (4\gamma_1\gamma_2/\gamma^2)$ is the linear resonant transmission of the PC defect, $\delta = (\omega_0\text{-}\omega)/\gamma$ is the frequency detuning of the input wave with respect to the defect mode. Due to the asymmetrical confinement ($\gamma_1 \neq \gamma_2$), the linear resonant transmission η is less than unity even in the lossless case.

When the input wave is launched from the right side, we can easily show that the expression for the transmission is the same as Eq. (3). However, the difference in the coupling of the input wave into the defect between the two launch directions (i.e. $\gamma_1 \neq \gamma_2$) leads to different nonlinear responses of the defect to the same external excitation. Thus, it is equivalent to think that for an asymmetrically confined PC defect the characteristic power p_0 is launch-direction-related. To show this more clearly, we can simplify the expression of p_0 given in Ref. [2] by omitting the parameters which are the same for the rightward and leftward launch directions, such as the resonant frequency, the Q factor of the defect mode, and the nonlinear refractive index. Also, it is noted that the contribution to the integrals involved in the formula mainly comes from the defect region. Using the coordinate shown in Fig. 1(a), we have

$$p_0 \sim \left[\int_{\text{Defect}} |F(x,z)|^2 \mathrm{d}x\mathrm{d}z\right]^2 \Big/ \left[\int_{\text{Defect}} |F(x,z)|^4 \mathrm{d}x\mathrm{d}z\right], \tag{4}$$

where $|F(x,z)|^2$ is the electric (or magnetic) field intensity for a defect mode with transverse electric (or magnetic) polarization whose electric (or magnetic) field is along y-axis. From Eq. (4), we can find that p_0 is very similar to the effective core area of an optical fiber that is determined by the modal distribution. Thus, if $|F(x,z)|^2$ is strongly concentrated in the defect region, then a low p_0 is expected. For an input wave with the same power density, the maximum values of $|F(x,z)|^2$ can be much different for the two launch directions. Since the input wave is easier to be coupled into the defect for the rightward launch direction, the peak value of $|F(x,z)|^2$ is found to be large, giving rise to a small p_0. Therefore, if we use p_{01} and p_{02} to represent the characteristics powers for the rightward and leftward input waves, then we have $p_{01} < p_{02}$ for the asymmetrically confined PC defect shown in Fig. 1(a). It is immediately realized that for the same input power p_{in}, the transmissions for the rightward and leftward input waves are different since Eq. (3) can be converted to

$$T = \frac{\eta}{1+\left[\left(p_{\text{in}}/p_0\right)T - \delta\right]^2}, \tag{5}$$

where p_0 takes p_{01} and p_{02} for the rightward and leftward input waves respectively. This is where the unidirectional transmission of an asymmetrically confined PC defect with nonlinearity comes from. More concretely, if we choose $(p_{02}/p_{01}) = 3$ and $\eta = 0.6$ for the asymmetrically confined defect, we can obtain the evolutions of the transmission spectra for the rightward and leftward launches with increasing the input power by using Eq. (5). The results are shown in Fig. 2 where the red and black curves represent the rightward and leftward launches, respectively. We present the transmission spectra for the two launch directions when the input power p_{in} is chosen to be 0.5 p_{01}, 2.0 p_{01}, 4.0 p_{01}, and 6.0p_{01}. Due to the nonlinear positive feedback effect, all of the spectra slant to the large-δ side (or to the low-frequency side). For each input power, the degree of slanting exhibits dependence on the launch direction. Since the input power is easier to be coupled into the defect from the left side, i.e. $p_{01} < p_{02}$, the spectrum slants more seriously and bistability of transmission appears firstly for the rightward launch, reflected in loop a→b→c→d→a that is shown in Fig. 2(c). Apparently, the section a→b→c can be employed to realize unidirectional transmission. In numerical simulations, this section can be observed by launching continuous waves (CWs)

#10367 - $15.00 USD Received 20 January 2006; revised 6 March 2006; accepted 6 March 2006

with different frequency detunings. On the other hand, we can obtain the section c→d→a by employing an input wave with a small positive frequency chirping, though it is useless for unidirectional transmission. The dotted branch in the middle of the loop is unstable and in general does not represent a real physical process.

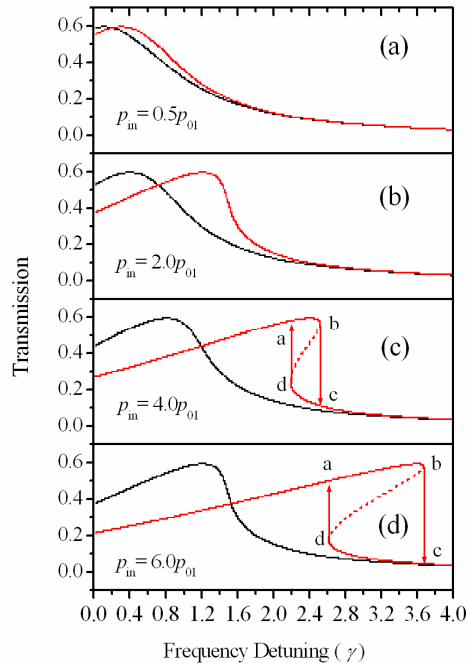

Fig. 2. Theoretical transmission spectrum of the single asymmetrically confined PC defect for the two launch directions and their evolutions with increasing input power. In the calculation, (p_{02}/p_{01}) and η are set as 3 and 0.6 respectively.

In this paper, what interests us mostly is the unidirectional transmission of the single and coupled PC defects. Considering the transmission spectra shown in Fig. 2(c), the transmission behavior of the PC defect can be divided into two types. When $\delta < \delta_0 \sim 1.2$, the transmission for the rightward input wave T_R is a little bit lower than that for the leftward one T_L. However, T_R becomes much larger than T_L for $\delta > \delta_0$ and before the down transition b→c occurs. Apparently, the input wave with frequencies in this region exhibits an unidirectional behavior. This region enlarges with increasing the input power. In general, the unidirectional transmission behavior can be described by the transmission contrast which is defined as $C = (T_R/T_L)$. More conveniently, we can use the maximum transmission contrast $C_{max} = (T_R/T_L)_{max}$ to characterize the efficiency of the resulting optical diodes. From Fig. 2, it seems that large C_{max} can be achieved by employing an input wave with a large δ and a high p_{in}.

As can be seen in Eq. (3), a high transmission can be obtained when δ is counteracted by (p_{out}/p_0). Obviously, the maximum value of T_R is the linear resonant transmission η. On the other hand, there exists a lower limit for T_L which is $\eta/(1+\delta^2)$ when $(p_{out}/p_{02}) << \delta$. Thus, it seems that the upper limit for C_{max} is $(1+\delta^2)$ when δ is decided. In order to get a large C_{max}, we need to use an input wave with a large δ, i.e., its frequency must be far from the resonant frequency of the defect mode. Such kind of input wave cannot be coupled into the defect unless its power is sufficiently high. Unfortunately, the dynamical shift of the defect mode we indicated recently suggests that the maximum transmission drops with increasing δ because it is actually the time-averaged value within an oscillation period of the defect mode [14]. Although Eq. (3) is simple and useful for describing the basic aspects of the nonlinear

#10367 - $15.00 USD Received 20 January 2006; revised 6 March 2006; accepted 6 March 2006

behavior of PC defects, we should keep in mind that the maximum transmission can be much smaller than η if a large δ and a high input power are employed. If the maximum transmission is very small, the unidirectional transmission will become meaningless. Therefore, increasing δ is not a correct way to enhance $C_{\max}$ and the unidirectional transmission is very limited when a single asymmetrically confined PC defect is employed. This point will be further verified later by numerical simulations.

3. Enhancement of transmission contrast through defect coupling

It is unfortunate that there exists a limitation when single PC defects are used to construct optical diodes. Nevertheless, the above analysis gives us a useful hint. If we can increase the order of δ in the transmission formula $\eta/(1+\delta^2)$, for instance, from 2 to 4, the lower limit of T_L will be further reduced to $\eta/(1+\delta^4)$, leading to an increase in $C_{\max}$. Of course, this can never happen for a single PC defect with a Lorentzian lineshape. However, it might be realized through defect coupling (or cascading) which has been utilized to achieve a lineshape with flat top and sharp sidewalls [15-17]. Therefore, it is worthy to investigate the structures consisting of two or more coupled PC defects.

In Fig. 1(b), we present a structure consisting of two PC defects that are coupled by an interconnecting waveguide whose length is $d–a$. If a large d is employed, the evanescent wave emerging from the left (or right) defect will eventually evolves into a guiding wave propagating in the slab waveguide within the frequency range of interest. In this case, the interconnecting waveguide only serves as a phase modulator for the guiding wave and no localization of wave occurs in it. Based on this structure, we can easily optimize the unidirectional transmission behavior by changing the value of d while remaining the decay rates of the constitutional defects. In Fig. 1(b), the right defect is exactly the same as the one shown in Fig. 1(a) while the left one is symmetrically confined with three air holes on both sides. Thus, the leftward and rightward decay rates of the mode amplitude for the left defect are equal to γ_1. Applying the CMT to the coupled defects [18-20], the linear transmission for the structure, as well as the involved parameters P_1~ P_4, can be expressed as

$$T = \frac{1}{P_1 + P_2(\delta + P_3)^2 + P_4(\delta + P_3)^4}, \tag{6}$$

$$\begin{cases} P_1 = \dfrac{\sin^2\varphi}{4\gamma_1^3\gamma_2}\left[(\gamma_1+\gamma_{01})(\gamma_2+\gamma_{02}) + \dfrac{\gamma_1^2}{\sin^2\varphi}\right]^2, \\ P_2 = \dfrac{\gamma^2\sin^2\varphi}{4\gamma_1^3\gamma_2}\left[(\gamma_1+\gamma_{01})^2 + (\gamma_2+\gamma_{02})^2 - \dfrac{2\gamma_1^2}{\sin^2\varphi}\right], \\ P_3 = \dfrac{\gamma_1}{\gamma\tan\varphi}, \text{ and } \quad P_4 = \dfrac{\gamma^4\sin^2\varphi}{4\gamma_1^3\gamma_2}. \end{cases} \tag{7}$$

Here, the meanings of γ_1, γ_2 and γ are the same as those mentioned in Sect. 2, γ_{01} and γ_{02} are the intrinsic decay rates of the mode amplitudes in the left and right defects respectively, φ ($\neq k\pi$, where k is an integer including zero) is the phase shift of the electromagnetic wave when it propagates between the two defects. The value of φ depends on the PC defects and the length of the interconnecting waveguide. It is confirmed that the lineshape of the structure with coupled defects will degenerate to a Lorentizian type $\eta/(1+\delta^2)$ if φ happens to be $k\pi$ [19]. It can be seen from Eq. (6) that the highest order of δ in the transmission formula is indeed increased to 4, though the transmission does not take exactly the form of $\eta/(1+\delta^4)$. What is more, it is found that the appearance of P_3 helps to reduce the transmission further if the condition of $\tan\varphi > 0$ is satisfied. Physically, P_3 arises from the linear coupling effect and it is often referred as the resonant frequency splitting. Thus, it is expected theoretically that T_L of the coupled PC defects is much lower than that of the single PC defect.

#10367 - $15.00 USD Received 20 January 2006; revised 6 March 2006; accepted 6 March 2006

4. Numerical simulation of linear transmission

In order to verify the analyses presented above, we first carry out linear FDTD simulations on the single asymmetrically and symmetrically confined PC defects. The lattice constant used in the simulations is a = 0.45μm. The width of the slab waveguide and the radius of air holes are chosen to be a and 0.3a, respectively. Since it has been confirmed that the simulation of a pure two-dimensional (2D) structure is a good approximation for the practical 2D PC slabs [21], we choose to simulate the TM defect mode of the 2D PC structure whose magnetic field is parallel to the air rods. The linear effective refractive index and the nonlinear coefficient of the slab waveguide are assumed to be 2.90 and 1.5×10^{-5} $\mu m^2/W$, respectively. The grid sizes in x- and z- directions and the boundary width of the perfectly matched layer for the simulations are set to be a/16 and a, respectively.

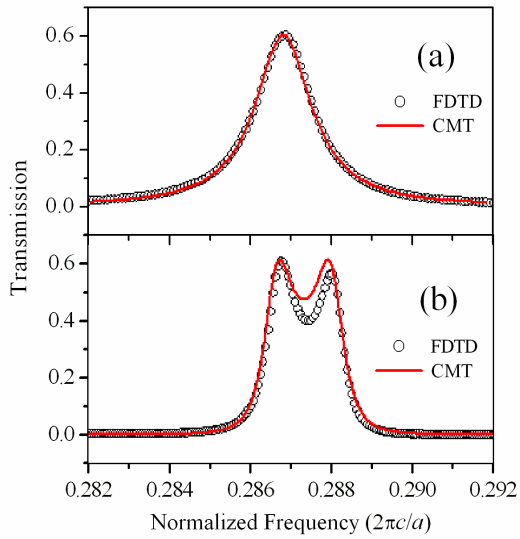

Fig. 3. Linear lineshapes of (a) the single asymmetrically confined PC defect and (b) two coupled PC defects calculated by the CMT (solid curves) and simulated by the FDTD (empty circles).

Under the very low input power, the asymmetrically confined PC defect shown in Fig. 1(a) exhibits a single defect mode located at $\omega_0 = 0.2869(2\pi c/a)$ or λ_0 = 1.568μm, where c is the speed of light in vacuum. The corresponding decay rates for the mode amplitude are measured numerically to be $\gamma_1 = 6.45\times10^{-4}$ $(2\pi c/a)$, $\gamma_2 = 1.69\times10^{-4}$ $(2\pi c/a)$, $\gamma_{01} = 0.35\times10^{-4}$ $(2\pi c/a)$, and $\gamma = 8.49\times10^{-4}$ $(2\pi c/a)$. The lineshape for the defect mode obtained by the numerical simulation is shown in Fig. 3(a) where the theoretical lineshape $\eta/(1+\delta^2)$ is also plotted by the red solid curve for comparison. For the symmetrically confined PC defect shown in the left side of Fig. 1(b), the resonant frequency is the same as $\omega_0 = 0.2869(2\pi c/a)$. In addition, the decay rates into the left and right waveguides are equal to $\gamma_1 = 6.45\times10^{-4}$ $(2\pi c/a)$ and the intrinsic decay rate of mode amplitude is derived to be $\gamma_{02} = 0.34\times10^{-4}$ $(2\pi c/a)$ which is almost the same as γ_{01}.

Similarly, we have measured numerically the linear transmission spectrum of the coupled structure in which d = 6.6a. Unlike the single defect, the spectrum possesses two peaks and sharp sidewalls, as shown in Fig. 3(b). Because of the narrow frequency region involved, the phase shift φ can be considered approximately as a constant. By setting φ as 0.31π, the theoretical spectrum based on Eq. (6) is in good agreement with the simulated one, as shown in Fig. 3(b). Here, the parameters P_1~P_4 appearing in Eq. (6) are calculated to be 2.10, -1.93, 0.52 and 1.96 by using Eq. (7). If the weak dependence of φ on ω is taken into account, the discrepancy between the theoretical spectrum and the simulated one can be eliminated.

#10367 - $15.00 USD Received 20 January 2006; revised 6 March 2006; accepted 6 March 2006

Furthermore, it is observed that the same spectrum appears when the value of d is increased to 7.4a, 8.1a or decreased to 5.9a, 5.2a. It verifies the theoretical result that the transmission spectrum of the coupled structure is a periodic function of φ, as reflected in Eqs. (6) and (7). In addition, it is found that the spectral shape shown in Fig. 3(b) remains nearly unchanged when the decay rates become smaller. For example, if we add one air hole on each side of the two defects, then we have four air holes on both sides of the left defect, and four and five air holes on the two sides of the right defect. In this case, we find that γ_1 and γ_2 decrease to be 1.69×10^{-4} ($2\pi c/a$) and 0.43×10^{-4} ($2\pi c/a$) respectively while γ_{01} and γ_{02} remain nearly unchanged. If the value of d is slightly reduced from 6.60a to 6.55a, then the similar spectral shape can be maintained though the linewidth is reduced to be one third of its original value. Unfortunately, the resonant transmission in this case is reduced to ~35%, which is much smaller than that shown in Fig. 3(b) (~62%), because the value of γ_2 approaches those of γ_{01} and γ_{02}. Hence, a much lower maximum transmission is expected for this structure which is not desirable for practical applications.

5. Numerical simulation of nonlinear transmission

In this paper, the simulations of the nonlinear transmission are completed by employing the nonlinear FDTD technique [22]. In order to simulate the unidirectional transmission behavior of the asymmetrically confined PC defect shown in Fig. 1(a), the CWs being the fundamental mode of the slab waveguide are launched into the structure from the left and right sides, respectively. Under different input powers, the transmission spectra for the two launch directions are obtained by scanning the frequency of the input wave while recording the corresponding transmission. The results are shown in Fig. 4 where the solid and the empty circles represent the rightward and leftward launches respectively. In each case, the maximum transmission C_{max} has been derived.

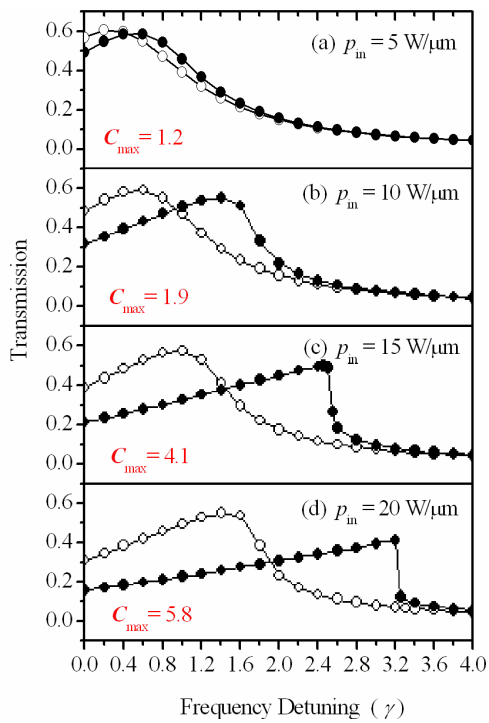

Fig. 4. Evolution of the transmission spectrum of the single asymmetrically confined PC defect with increasing input power. The solid and empty circles represent the rightward and leftward launch cases respectively.

#10367 - $15.00 USD Received 20 January 2006; revised 6 March 2006; accepted 6 March 2006

A detailed comparison of Fig. 4 and Fig. 2 indicates that the simulated results are in good agreement with the theoretical one except the maximum transmission. Since we use input waves without any frequency chirping, the transmission breaks shown in Fig. 4 correspond to the down transition b→c shown in Fig.2, not the up transition d→a. It can be seen that the maximum transmission drops with the increase of the input power, especially in the rightward launch direction. It supports the existence of the dynamical shift effect, as we have mentioned in Sect. 2. Since the input power is easier to be coupled into the defect via the rightward launch, the corresponding shift of the defect mode is larger. Accordingly, the reduction in the maximum transmission is also larger. This feature becomes more obvious at high input powers. In the case of p_{in} = 15W/μm, we have C_{max} = 4.1 and T_R = 52% (~0.85η), as shown in Fig. 4(c). When p_{in} is further raised to 20W/μm, we observe that C_{max} increase to 5.8 but T_R drops to 43% (~0.70η), as shown in Fig. 4(d). Based on this phenomenon, we can understand why the unidirectional transmission of single PC defects is very limited.

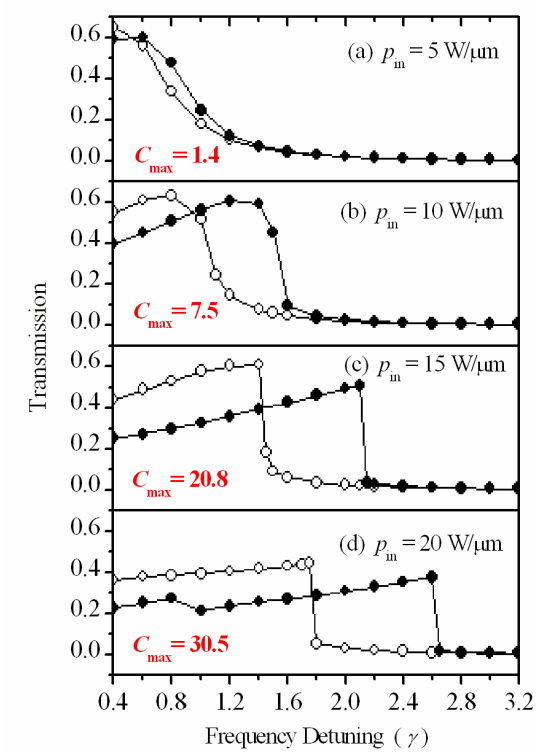

Fig. 5. Evolution of the transmission spectrum of the two coupled PC defects with increasing input power. The solid and empty circles represent the rightward and leftward launch cases respectively.

Now we turn to the structure consisting of two coupled defects shown in Fig. 1(b), using the same procedure to simulate its nonlinear transmission behavior. The results are presented in Fig. 5. At first glance, the transmission spectra for both launch directions exhibit similar evolutions to those observed in the single PC defect shown in Fig. 4. However, a detailed inspection reveals that the region showing unidirectional transmission looks like a rectangle rather than the triangle found in Fig. 4. It implies that a significant enhancement in the transmission contrast has been achieved in the coupled PC defects. In Fig. 5, we find that C_{max} = 20.8, T_R = 51% (~0.84η) at p_{in} = 15 W/μm and C_{max} = 30.5, T_R = 38% (~0.62η) at p_{in} = 20 W/μm. As compared with the single PC defect, the transmission contrast is enhanced by one

#10367 - $15.00 USD Received 20 January 2006; revised 6 March 2006; accepted 6 March 2006

order of magnitude while the maximum transmission remains nearly unchanged. It confirms that the linear coupling effects do improve greatly the unidirectional transmission behavior. We have also examined other coupled defect structures with different values of d. In all cases, similar results to the case of $d = 6.6a$ are observed and all show better performance than the single PC defect case. More interestingly, we find that the evolutions of the transmission spectrum are almost the same when d is chosen to be $5.2a$, $5.9a$, 6.6a, $7.4a$ and $8.1a$.

Being more practical than the CW case, let us examine the unidirectional transmission behavior of the coupled defect structure for a Gaussian pulse of 3 ps. Based on the results in the CW case shown in Fig. 5, we expect that a nice unidirectional propagation can be realized by choosing: (i) $\delta = 2.0$, i.e., the carrier frequency for the pulse is $\omega = 0.2852(2\pi c/a)$, and p_{in} = 16W/μm, where p_{in} is the input peak power; or (ii) $\delta = 2.5$, i.e., $\omega = 0.2848(2\pi c/a)$, and p_{in} = 21 W/μm. In Fig. 6, we present the simulated results in time domain for both cases that have been normalized by the input peak power. Here, the transmission contrast C is defined as the ratio of the rightward output peak power to the leftward one. Apparently, very good unidirectional propagations have been realized in both cases. In Fig. 6(a), we find a lower contrast (~ 14.6) and a higher transmission (~ 40.3%). In Fig. 6(b), it can be seen that the contrast (~ 21.3) is enhanced at the expense of the transmission (~ 30.5%).

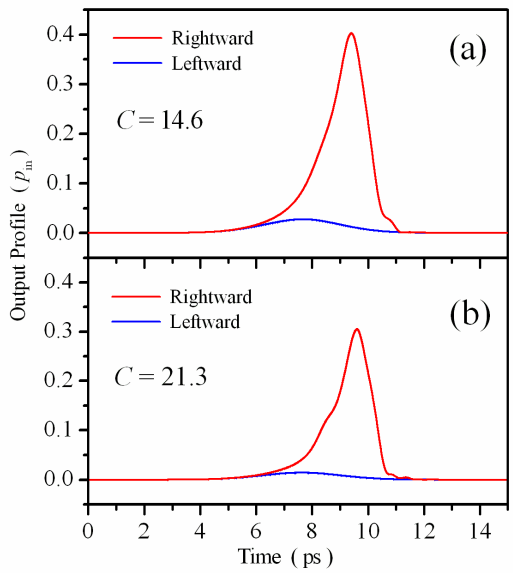

Fig. 6. Unidirectional transmission behavior of the two coupled PC defects for a Gaussian pulse of 3 ps under two different launch conditions. (a) $\delta = 2.0$, p_{in} = 16W/μm and (b) $\delta = 2.5$, p_{in} = 21W/μm.

6. Conclusion

In summary, we investigate the unidirectional transmission behavior of PC defects with nonlinearity and concentrate on the issue of improving the transmission contrast by using the coupled defect structure. An analytical expression for the transmission based on the nonlinear CMT, which is difficult to derive, is very important for fully understanding the transmission contrast of the coupled defects. However, we reveal that the maximum transmission contrast of the coupled defects depends mainly on the linear coupling effects, such as the highest order of the frequency detuning and the frequency splitting when two coupled defects are involved, although the asymmetric configuration and nonlinearity are the intrinsic physical origins of the unidirectional transmission behavior. Our theoretical analyses are in good agreement with the simulation results based on the finite-difference time-domain technique. A significant

#10367 - $15.00 USD Received 20 January 2006; revised 6 March 2006; accepted 6 March 2006

enhancement in the transmission contrast by an order of magnitude has been achieved by employing two coupled PC defects.

Acknowledgments

The authors acknowledge the financial support from the National Natural Science Foundation of China (Grant No. 10374065). One of the authors (S. Lan) would like to thank the financial support by the Program for New Century Excellent Talents in University of China.

#10367 - $15.00 USD Received 20 January 2006; revised 6 March 2006; accepted 6 March 2006